ISBN: 978-3-95450-231-8 ISSN: 2673-5490 doi: 10.18429/JACoW-IPAC2023-THPL110

A CONSECUTIVE DOUBLE-SLIT EMITTANCE METER FOR HIGH-BRIGHTNESS ELECTRON SOURCE*

R. Yang†, W. Chen, W. Huang, S. Jiang, R. Liu, T. Yang, S. Wang
Institute of High Energy Physics, 100049 Beijing, China
also at China Spallation Neutron Source, 523000 Dongguan, China

Abstract

High-brightness photoinjector has been an indispensable electron source driving X-ray free electron lasers (FEL). To improve the performance of the next-generation FEL, a high-quality electron beam with a small emittance, e.g., 0.1 mm.mrad for a 100 pC bunch charge, will be of vital importance. A consecutive double-slit emittance meter has been proposed to measure such a small-emittance beam with satisfactory accuracy. Analytical evaluations and optimizations have been performed based upon the beam parameters of a C-band photocathode RF gun being constructed in the China Spallation Neutron Source (CSNS).

INTRODUCTION

To improve the brightness of the next generation FELs, a high-brightness electron source providing a small-emittance beam, e.g., 0.1 mm.mrad for a bunch charge of 100 pC, will be of vital importance. A C-band photocathode RF gun with a gradient of more than 150 MV/m can quickly improve beam energy to relativistic energy and effectively suppress the undesired emittance growth due to space-charge forces [1-5]. Comparing with the X-band photocathode RF gun, the C-band RF gun has a reasonable dimension that reduces the critical requirements on the manufacture precision. Thanks to the merit of a higher accelerating gradient with controllable fabrication difficulty, the high-brightness C-band photoinjector has been proposed for future FELs in several institutes.

For the demonstration of the key techniques for future FEL facilities, a photoinjector test stand has been constructed in the Chinese Spallation Neutron Source campus. This test beam consists of a driven laser, a 3.6-cell C-band RF gun, and downstream diagnostics instruments, as shown in Fig. 1. Concerning the merit of a long lifetime and promising tolerance on the vacuum, the copper cathode has been used. As a consequence, a 266 nm UV laser with a repetition rate of 0-100 Hz, a pulse energy of 2 mJ, and a pulse width (FWHM) of less than 0.8 ps has been developed. The prototype C-band RF gun has been manufactured and an electric field of 150-180 MV/m on the copper cathode has been confirmed in the cold test. The typical beam parameters have been summarized in TABLE. 1. The beam instrumentations include an integrating current transformer (ICT), an emittance meter, an energy spectrometer, and a Faraday cup. The designed sensitivity of the ICT is 5 Vs/C with an output gain of 20 dB and pulse width of about 70 ns. To quantify the energy spectrum, two slits of a width of 50 μm and with a gap of 100 mm in between forming a vertical collimator have been placed in front of the bending magnet. The momentum profile is then determined by the transverse image at the downstream screen with the known dispersion obtained from ASTRA simulation. Since the ICT is an indirect diagnostic and demands periodic recalibration, a Faraday cup has been designed for direct current measurement with high accuracy. To cure the escaping of backscattered particles, a bias voltage of 1 kV will be applied at the cup entrance. With careful optimization of the geometry, a capacity of about 15.6 pF has been achieved in simulation which enables registering signal with satisfactory precision.

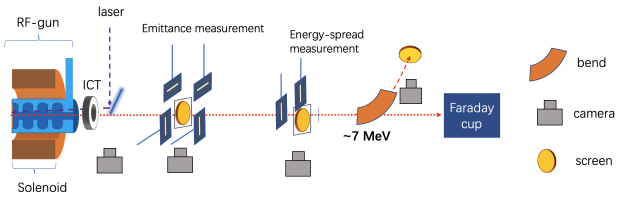

Figure 1: Schematic of the C-band photoinjector test stand at CSNS.

Table 1: Design Parameters of the C-band Photoinjector Test Stand at CSNS.

Parameter	Unit	Value
RF frequency	GHz	5.712
Accelerating gradient	MV/m	150
Repetition rate	Hz	1-100
Beam energy at the gun exit	MeV	7.3
Bunch charge	nC	0.1~1
Transverse emittance (0.1 nC)	mm.mrad	<0.2
Bunch length	ps	5

To achieve the expected small-emittance beam, the diagnostic probe, emittance model and automatic optimization scheme are necessary. Although the beam is at the relativistic energy at the exit of the photocathode RF gun, the space-charge force is still a major obstacle for accurate emittance diagnostics. For the emittance measurements employing the conventional single-slit scan, multi-slit method, or pepper-pot method, a micrometer-scale slit width or hole diameter allowing an extra-small partition of particles to pass through is required. This brings grand challenges to state-of-art manufacture and alignment techniques. To tackle the

* WORK SUPPORTED BY GUANGDONG BASIC AND APPLIED BASIC RESEARCH FOUNDATION (2022A1515140179).
† yangrenjun@ihep.ac.cn

ISBN: 978-3-95450-231-8 ISSN: 2673-5490 doi: 10.18429/JACoW-IPAC2023-THPL110

above challenges, a novel emittance meter capable of accurate measurements of small emittance and with reasonable fabrication and assembly difficulty has been proposed and designed for the C-band photocathode test stand.

DESIGN CONSIDERATIONS

For the reconstruction of the phase-space profile and emittance, the suppression of the space-charge forces, beamlet imagination and algorithm for space-space analysis are key considerations [6-12].

Thanks to the technical recipes for the single-slit-based emittance meter in Ref. [7], a tungsten slit mask of a thickness of 2 mm, which provides sufficient angle acceptance and beam stop/scattering performance, has been chosen. To evaluate the influence of the space-charge force, a space-charge dominance ratio for the beamlet is typically employed. Here, we have alternatively assessed the impact of space-charge forces through tracking simulations in ASTRA concerning the design beam parameters. In the simulation, beamlets are imagined at 0.55 m downstream of the slit mask and then integrated for the determination of beam size. In the absence of space-charge force, the beam sizes are slightly lower than the expectations due to the angle acceptance. In the presence of space-charge force, a single slit width of ~5, 15~20 and 30~50 μm is required for a bunch charge of 0.1, 0.3 and 0.5 nC, as shown in Fig. 2. The latter two slit widths are technically feasible, however, a slit width of about 5 μm is difficult to fabricate.

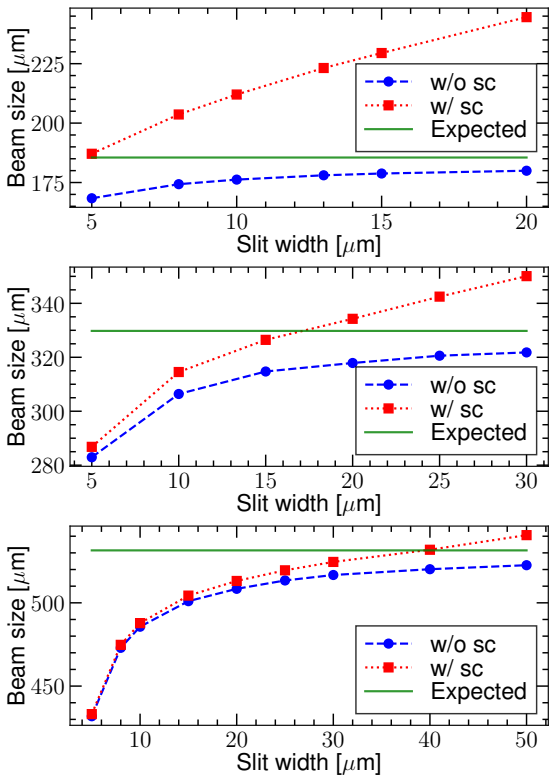

Figure 2: Beam sizes at the downstream screen(~0.55 m) for a bunch charge of 0.1, 0.3 and 0.5 nC.

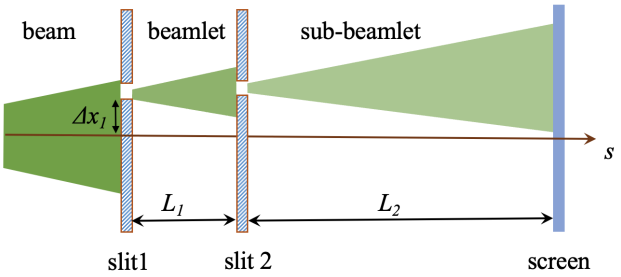

Figure 3: Principle of the consecutive double-slit emittance meter.

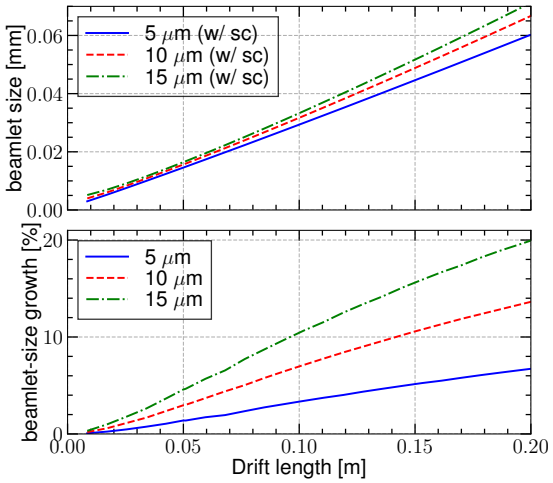

Figure 4: Beamlet sizes and its growth rate (comparing with the expectations without space-charge force) as a function of the drift length in the presence of space-charge force.

During the beamlet spreading between the front slit and downstream profile monitor, the dilution due to space charge is related to the particle population and impacting time. Instead of single-slit scanning with an extra-small slit width, a consecutive double-slit scan has been proposed for measuring the small emittance (<0.2 mm.mrad). As shown in Fig. 3, the beamlet produced by the front slit is shaped into sub-beamlets by the latter slit located at L_1 downstream. Assuming two slits with similar widths, the initial sizes of the beamlet and sub-beamlet are comparable. But, the space charge of the sub-beamlet is much lower owing to a very small particle population. The distance between these two slits is determined by the compromise among the strength of space charge force, the fabrication difficulty of the slit mask and the sensitivity of the sub-beamlet imaging system. The upper limit of the width of the second slit is given by the beamlet size, and the bottom limit is determined by the fabrication difficulty. Since the space-charge force is extremely weak for the sub-beamlet, the distance of the drift from the latter slit to the screen (L_2) should be determined concerning the resolution of the imaging system.

Concerning the beam parameters at a bunch charge of 0.1 nC, the beamlet-size growth has been evaluated for a front slit width of 5, 10 and 15 μm, as shown in Fig. 6. With

ISBN: 978-3-95450-231-8 ISSN: 2673-5490 doi: 10.18429/JACoW-IPAC2023-THPL110

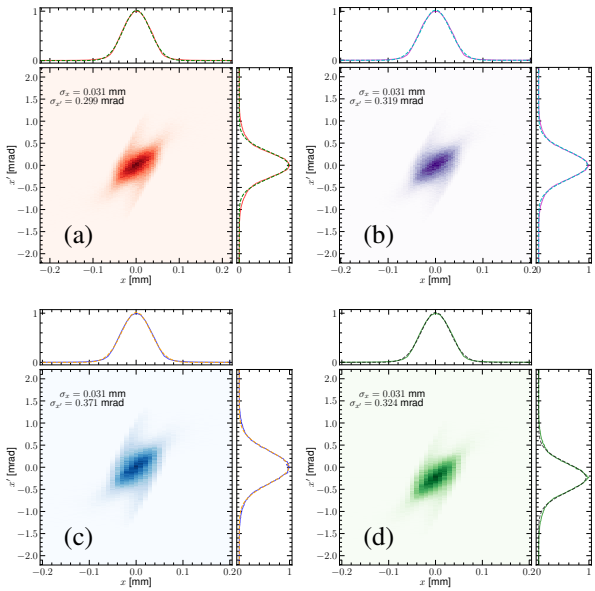

Figure 5: Expected phase-space profile at the first slit (a), phase-space profiles constructed from beamlet intensity distributions with slit widths of 5 and 10 μm (b, c) and phase-space profile determined by sub-beamlet profiles with slit widths of 10 μm (d).

a front slit width of 10 μm, the gap between the two slits is set as 0.1 m inducing a beamlet-size growth of ~7% than that in the absence of space-charge force. Regarding a small beamlet at the second slit (~30 μm), a slit width of 10 μm has been chosen. Thus, the beamlet is then divided into ~9 sub-beamlets. To loose the requirements of the resolution of the imaging system, a drift length of 0.75 m providing a sub-beamlet size of 30~40 μm at the screen has been implemented to L_2. With linear transfer matrices, the phase-space profiles have been reconstructed with single-slit and consecutive double-slit scans, as shown in Fig. 5. For a single-slit width of 5 μm and the consecutive double-slit widths of 10 μm, the constructed rms beam divergences are about 8% higher than the expectation. But, the rms beam divergence grows by 24% constructed by the single-slit scan with a slit width of 10 μm.

TOWARDS EXPERIMENTAL DEMONSTRATION

Following the above design considerations and constraints, an emittance meter has been designed at CSNS. At the first slit mask, multiple slit widths of 10, 20 and 50 μm and a Ce:YAG screen are arranged capable for emittance measurements at a bunch charge of 0.1-0.5 nC and beam profile imaging. In the downstream, the other mask with a slit width of 10 μm is inserted. For the beamlet and sub-beamlet imagination, a Ce:YAG screen, a 45° mirror and an in-air optical observation system are employed. Such configuration has the merit of excellent resolution, smaller than the Ce:YAG screen and the transition radiation light generated at the mirror has been verified to be negligible. On the other hand, this beamlet imaging system has been integrated with the slit masks for energy spectrum measurement. Concerning diffraction limit, screen thickness, pixel size and optical aberration of the macro zoom lens, a spatial resolution of about 10 μm has been predicted.

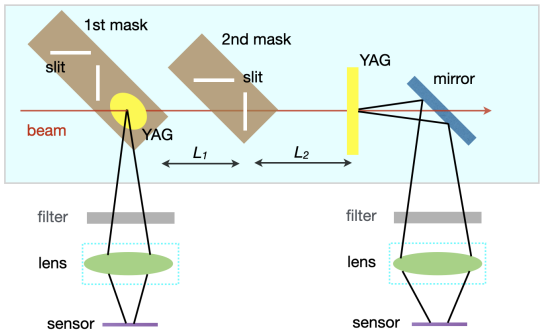

Figure 6: Schematic of the emittance meter for the C-band photocathode test stand at CSNS.

In addition, the actual slit widths of 9.08±0.73, 20.76±0.73 and 50.59±0.47 has been checked using a microscope, as shown in Fig. 7.

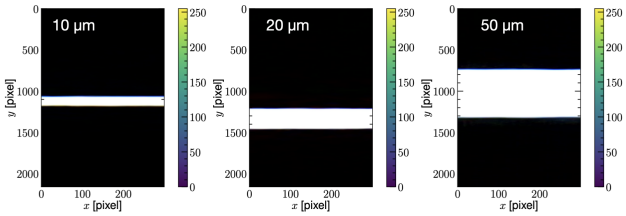

Figure 7: False color images of slits obtained with a 50X microscope. Notice that one pixel represents 0.085 μm.

CONCLUSIONS

To quantify the emittance of the high-brightness electron source required for next-generation FELs, a consecutive double-slit emittance meter has been proposed and designed with respects to the designed beam parameters of a C-band photoinjector test stand at CSNS. Major considerations and constraints towards an accurate emittance measurement have been described in detail. The experimental demonstrations will be conducted after assembly and commissioning of the photoinjector test stand.

REFERENCES

[1] M. Ferrario *et al.*, "Direct Measurement of the Double Emittance Minimum in the Beam Dynamics of the Sparc High-Brightness Photoinjector", *Phys. Rev. Lett.* vol. 99, no. 23, p. 234801, Dec. 2007. doi:/10.1103/PhysRevLett.99.234801

[2] M. Schaer *et al.*, "Study of a C-band TW electron gun for SwissFEL", in *Proc. IPAC'14*, Dresden, Germany,

ISBN: 978-3-95450-231-8 ISSN: 2673-5490 doi: 10.18429/JACoW-IPAC2023-THPL110

May 2014, paper MOPRI043, pp. 686-688. doi:10.18429/JACoW-IPAC2014-MOPRI043

[3] M. Croia *et al.*, "High gradient ultra-high brightness C-band photoinjector optimization", *J. Phys.: Conf. Ser.* vol. 1596, p. 012031, 2020. doi:10.1088/1742-6596/1596/1/012031

[4] L. Wang *et al.*, "Design, fabrication and cold-test results of a 3.6 cell C-band photocathode RF gun for SXFEL", *Nucl. Instr. Meth. A*, vol. 1003, p. 165320, 2021. doi:10.1016/j.nima.2021.165320

[5] X. Liu *et al.*, "A C-band test platform for the development of RF photocathode and high gradient accelerating structures", presented at IPAC'23, Venice, Italy, May 2023, paper MOPA181, this conference.

[6] M. Zhang, "Emittance Formula for Slits and Pepper-pot Measurements", Rep., FermiLab-TM-1988, Oct. 1996.

[7] S. G. ANDERSON *et al.*, "Space-charge effects in high brightness electron beam emittance measurements", *Phys. Rev. ST Accel. Beams*, vol. 5, p. 014201, Jan. 2002. doi:10.1103/PhysRevSTAB.5.014201

[8] K. Togawa *et al.*, "CeB6 electron gun for low-emittance injector", *Phys. Rev. ST Accel. Beams*, vol. 10, p. 020703, Feb. 2007. doi:10.1103/PhysRevSTAB.10.020703

[9] L. Yan *et al.*, "Multislit-Based Emittance Measurement of Electron Beam from a Photocathode Radio-Frequency Gun", *Chinese Phys. Lett*. vol. 25, pp.1640-1643, May 2008. doi:10.1088/0256-307X/25/5/032

[10] C. Liu *et al.*, "Transverse Beam Emittance Measurements with Multi-Slit and Moving-Slit Devices for LEReC", in *Proc. IBIC2018*, Shanghai, China, Aug. 2018, paper WEPB21, pp.486-489. doi:10.18429/JACoW-IBIC2018-WEPB21

[11] R. Niemczyk *et al.*, "Slit-Based Slice Emittance Measurements Optimization at PITZ", in *Proc. IBIC2019*, Malmö, Sweden, Sep. 2019, paper TUPP013, pp.1-3. doi:10.18429/JACoW-IBIC2019-TUPP013

[12] H. Qian *et al.*, "Analysis of photoinjector transverse phase space in action and phase coordinates", *Phys. Rev. Accel. Beams*, vol. 25, p. 103401, Oct. 2022. doi:10.1103/PhysRevAccelBeams.25.103401